Research Article **Open Access**

Stephen E. Moore*, Hetsron L. Nyandjo-Bamen, Olivier Menoukeu-Pamen, Joshua Kiddy K. Asamoah, and Zhen Jin

Global stability dynamics and sensitivity assessment of COVID-19 with timely-delayed diagnosis in Ghana

https://doi.org/10.1515/cmb-2022-0134
Received February 9, 2022; accepted May 16, 2022

Abstract: In this paper, we study the dynamical effects of timely and delayed diagnosis on the spread of COVID-19 in Ghana during its initial phase by using reported data from March 12 to June 19, 2020. The estimated basic reproduction number, $\mathcal{R}_0$, for the proposed model is 1.04. One of the main focus of this study is global stability results. Theoretically and numerically, we show that the disease persistence depends on $\mathcal{R}_0$. We carry out a local and global sensitivity analysis. The local sensitivity analysis shows that the most positive sensitive parameter is the recruitment rate, followed by the relative transmissibility rate from the infectious with delayed diagnosis to the susceptible individuals. And that the most negative sensitive parameters are: self-quarantined, waiting time of the infectious for delayed diagnosis and the proportion of the infectious with timely diagnosis. The global sensitivity analysis using the partial rank correlation coefficient confirms the directional flow of the local sensitivity analysis. For public health benefit, our analysis suggests that, a reduction in the inflow of new individuals into the country or a reduction in the inter community inflow of individuals will reduce the basic reproduction number and thereby reduce the number of secondary infections (multiple peaks of the infection). Other recommendations for controlling the disease from the proposed model are provided in Section 7.

Keywords: Epidemiology of COVID-19; Lyapunov function; Latin hypercube sampling; Ghana

MSC: 34D23; 37N25; 92-10

1 Introduction

COVID-19 was declared a pandemic in the first quarter of 2020 by the World Health Organization (WHO) see, e.g. [1]. The disease affects different people in different ways with most infected people developing mild to moderate illness. Most common symptoms are fever, dry cough and tiredness while less common symptoms include aches and pains, sore throat, diarrhoea, conjunctivitis, headache, loss of taste or smell, a rash on skin or discolouration of fingers or toes [1, 3]. It is well understood that the elderly with underlying medical

***Corresponding Author: Stephen E. Moore:** Department of Mathematics, University of Cape Coast, Ghana
Regional Transport Research and Education Centre Kumasi, Kwame Nkrumah University of Science andTechnology, Kumasi, Ghana, E-mail: stephen.moore@ucc.edu.gh
Hetsron L. Nyandjo-Bamen: African Institute for Mathematical Sciences, Ghana
Department of Mathematics, School of Science, College of Science and Technology, University of Rwanda, Rwanda
Olivier Menoukeu-Pamen: African Institute for Mathematical Sciences, Ghana
IFAM, Department of Mathematical Sciences, University of Liverpool, United Kingdom
Zhen Jin: Complex Systems Research Center, Shanxi University, Taiyuan 030006, China
Joshua Kiddy K. Asamoah: Department of Mathematics, Kwame Nkrumah University of Science andTechnology, Kumasi, Ghana

problems are the most vulnerable people. COVID-19 is transmitted by means of contact (direct or indirect), droplet spray in short range transmission and aerosol in long-range transmission (airborne transmission) [2]. Globally, there were 100, 285, 517 confirmed cases with 2, 149, 461 confirmed death cases as on 26th January, 2020 [3].

In Africa, there were a total of 3, 472, 023 confirmed cases with 86, 060 confirmed death cases where Ghana is among the top ten (10) most infected countries as on 26th January, 2021 [3]. As on 26th January, 2021, Ghana had 62, 135 confirmed cases with 372 confirmed death cases. The first confirmed cases in Ghana were recorded on 12th of March, 2020 from two people who had returned from Norway and Turkey [4]. In Figure 1, we presented the logistic growth model for the cumulative cases of COVID-19 for Ghana on 25th January, 2021.

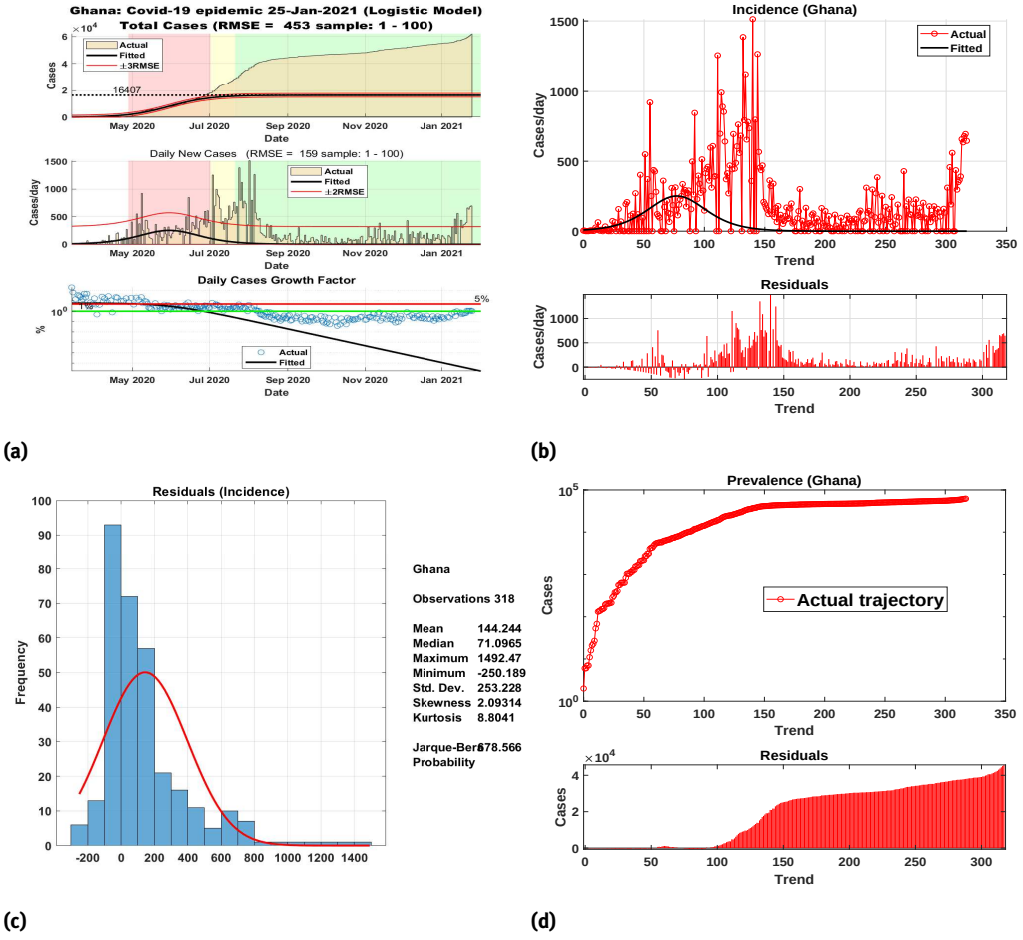

Figure 1: Logistic model fit and cumulative trajectories for reported cases for Ghana.

Several works have been studied concerning COVID-19 including a human-to-human model analysis comparing Ghana and Egypt [5–9]. The transmission dynamics in Wuhan has also been studied and presented in several articles with control measures and basic reproduction number well analyzed, see e.g. [10–12]. In [13], the authors analyzed COVID-19 spread dynamics with environmental influence using the reported cases in Ghana. Most recently, a modified SEIR compartmental model with nine compartments (CoVCom9) to describe the dynamics of SARS-CoV-2 transmission in Ghana has also been developed with a detailed mathematical analysis including the derivation of the basic reproduction number, see, [14]. Also, a COVID-19 model that accounts for the symptomatic, asymptomatic and hospitalized people has been presented with optimal cost-effective control measures with data from Nigeria, see, [15]. Other COVID-19 models have been developed

and analysed for other African countries like Cameroon, Togo, Gabon, etc., see, e.g. [16–18]. In [19], the control strategies to curb the virus using data from Wuhan were presented. Measures to control the spread of COVID-19 are mostly avoiding human-to-human contacts, personal protection and environmental disinfection. The diagnosis of COVID-19 is difficult and the incubation period of $2-14$ days or $0-24$ days is longer than most known coronaviruses or similar viruses which usually ranges between 1 to 10 days [20]. Due to the long incubation period, it results in a delay in diagnosis. This delay allows for human-to-human transmission as well as human-environment-human transmission. In this article, we present the transmission dynamics of COVID-19 considering human-environment-human dynamics for Ghana. We have mainly considered Ghana from the anglophone west Africa to understand the effect of timely-delayed dynamics in these region in the sub-saharan continent. For mathematical feasibility, we will present the global stability analysis, the basic reproduction numbers, sensitivity assessment and numerical simulations of the proposed model.

The rest of the article is organized as follows; In Section 2, we present the model formulation and definition of parameters used. Section 3 concerns the existence and uniqueness as well as the positivity and boundedness of the solution. We present the analysis of disease-free equilibrium in Section 4 and the endemic equilibrium in Section 5. The numerical results using data from Ghana and corresponding parameters are presented in Section 6. We present local and global sensitivity analysis in section 7. Finally, the concluding remarks and recommendations are presented in Section 8.

2 Model formulation

The delay in diagnosis of COVID-19 leads to an increase in the spread of the virus. In all teaching hospitals in Ghana, patients are required to be tested for COVID-19 before any major treatment can be effected. Also, the delay in the diagnosis impacted on the severity of several diseases including pulmonary diseases [21, 22]. Rong et al.[10] studied the impact of delay in diagnosis on the spread of covid-19 in Wuhan. Our interest is to modify their model for the case of Ghana. Based on the model formulated in [10], we propose a modified version of the epidemiological compartment model that takes into account the recruitment of hosts as a result of people traveling in and out of Ghana during the initial phase of the pandemic and the natural death of people due to other factors. Here, we note that the total human population size denoted as (N) is divided into susceptible (S), self-quarantine susceptible (S_q), exposed (E), infectious with timely diagnosis (I_1), infectious with delayed diagnosis (I_2), hospitalized (H) and recovered (R). The viral spread in the environment is denoted as (V). Hence for the total human population at time t we have $N(t) = S(t)+S_q(t)+E(t)+I_1(t)+I_2(t)+H(t)+R(t)$. We also consider that all parameters are positive and it is only the I_1, I_2 and H compartments which experiences disease induced death at a rate, d. The overall force of infection is given as $\lambda = \beta_e E + \beta_{i_1} I_1 + \beta_{i_2} I_2 + \beta_v V$. We refer the interested reader to reference [10] for detailed explanations for the remainder of model parameters.

Figure 2 below shows the compartment model describing the interaction between the human population and the pathogens in the environment.

The description of the parameters used in the model for the COVID-19 transmission are given in Table 1. Following the compartmental transition diagram as shown in Figure 2, the eight state dynamical model describing the transmission dynamics of COVID-19 is given by

$$\begin{aligned}
\frac{dS}{dt} &= \Lambda - \lambda S + q_1 S_q - (\mu + q)S,\\
\frac{dS_q}{dt} &= qS - q_1 S_q - \mu S_q,\\
\frac{dE}{dt} &= \lambda S - \omega E - \mu E,\\
\frac{dI_1}{dt} &= \phi\omega E - \gamma_1 I_1 - \mu I_1 - dI_1,\\
\frac{dI_2}{dt} &= (1-\phi)\omega E - \gamma_2 I_2 - \mu I_2 - dI_2,\\
\frac{dH}{dt} &= \gamma_1 I_1 + \gamma_2 I_2 - mH - \mu H - dH,
\end{aligned} \tag{1}$$

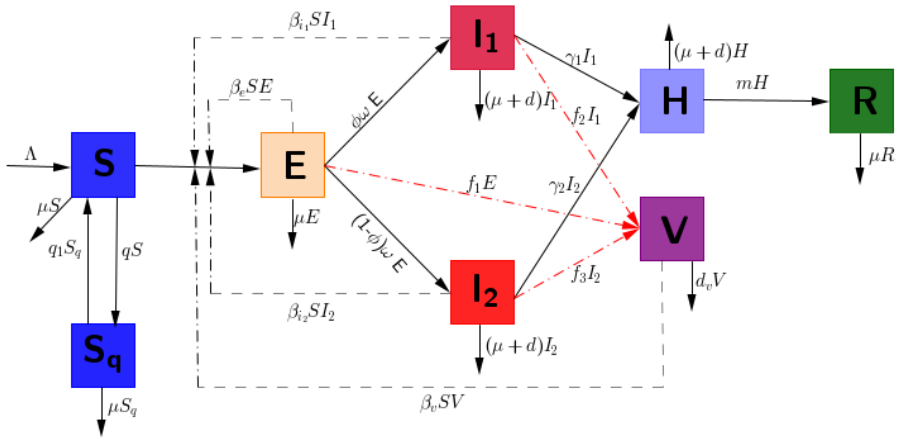

Figure 2: Diagram of COVID-19 Dynamics.

Table 1: Description of parameters.

Parameter	Description
Λ	Recruitment rate
q	Self-quarantined rate of the susceptible
q_1	Transition rate of self-quarantined individuals to the susceptible
β_e	Transmission rate from the exposed to the susceptible
β_{i_1}	Transmission rate from the infectious with timely diagnosis to the susceptible
β_{i_2}	Transmission rate from the infectious with delayed diagnosis to the susceptible
β_v	Transmission rate from the susceptible to the exposed (infected by virus)
$1/\omega$	Incubation period
ϕ	Proportion of the infectious with timely diagnosis
$1/\gamma_1$	Waiting time of the infectious for timely diagnosis
$1/\gamma_2$	Waiting time of the infectious for delayed diagnosis
μ	Natural human death rate
d	Disease-induced death rate
m	Recovery rate of the hospitalized
f_1	Virus released rate of the exposed
f_2	Virus released rate of the infectious with timely-diagnosis
f_3	Virus released rate of the infectious with delayed-diagnosis
d_v	Decay rate of virus in the environment

$$\frac{dR}{dt} = mH - \mu R,$$
$$\frac{dV}{dt} = f_1 E + f_2 I_1 + f_3 I_2 - d_v V.$$

3 Analysis of the model problem

The model (1) is described by a system of first order autonomous nonlinear differential equations. It can be rewritten in the matrix form as

$$X'(t) = F(X(t)), \tag{2}$$

where $X(t) := (S, S_q, E, I_1, I_2, H, R, V)^T$ and F is a smooth function defined from $\mathbb{R}^8$ by

$$F(X) := \begin{pmatrix} \Lambda - (\beta_e E + \beta_{i_1} I_1 + \beta_{i_2} I_2 + \beta_v V)S + q_1 S_q - (\mu + q)S \\ qS - q_1 S_q - \mu S_q \\ (\beta_e E + \beta_{i_1} I_1 + \beta_{i_2} I_2 + \beta_v V)S - \omega E - \mu E \\ \phi\omega E - \gamma_1 I_1 - \mu I_1 - dI_1 \\ (1-\phi)\omega E - \gamma_2 I_2 - \mu I_2 - dI_2 \\ \gamma_1 I_1 + \gamma_2 I_2 - mH - \mu H - dH \\ mH - \mu R \\ f_1 E + f_2 I_1 + f_3 I_2 - d_v V \end{pmatrix},$$

where $X := (S, S_q, E, I_1, I_2, H, R, V) \in \mathbb{R}^8$. Since F is a smooth function, then F is locally lipschitz on $\mathbb{R}^8$. And we deduce the existence and uniqueness of the maximal solution to the Cauchy problem associated with the differential system (1) relating to the initial condition $(t_0, X_0) \in \mathbb{R} \times \mathbb{R}^8$.

Next, we consider the positivity of the solution. Here, we investigate the asymptotic behavior of orbits starting in the non-negative cone $\mathbb{R}^8_+$.

Theorem 3.1. *For any initial condition* $\left(t_0 = 0, X_0 = (S(0), S_q(0), E(0), I_1(0), I_2(0), H(0), R(0), V(0)) \in \mathbb{R}^8_+\right)$, *the maximal solution* $\left([0, T[|X(t) = (S(t), S_q(t), E(t), I_1(t), I_2(t), H(t), R(t), V(t))\right)$ *of the Cauchy problem related with system* (1) *is non-negative.*

Proof. We define the set $\Delta := \left\{\widetilde{t} \in [0, T[\mid X(t) > 0, \ \forall t \in]0, \widetilde{t}[\right\}$. Since $(S, S_q, E, I_1, I_2, H, R, V)$ are continuous functions, then $\Delta \neq 0$. Also, let $\widetilde{T} := \sup \Delta$ and show that $\widetilde{T} = T$. Assume $\widetilde{T} < T$, then $S, S_q, E, I_1, I_2, H, R$ and V are simultaneously positive on $]0, \widetilde{T}[$.

At least one of the following conditions is satisfied at time $\widetilde{T}$: $S(\widetilde{T}) = 0$, $S_q(\widetilde{T}) = 0$, $E(\widetilde{T}) = 0$, $I_1(\widetilde{T}) = 0$, $I_2(\widetilde{T}) = 0$, $H(\widetilde{T}) = 0$, $R(\widetilde{T}) = 0$ or $V(\widetilde{T}) = 0$.

Assume $S(\widetilde{T}) = 0$, then we deduce from the first equation of system (1)

$$\frac{d}{dt}\left(Se^{\int_0^t(\lambda(s)+\mu+q)ds}\right) = (\Lambda + q_1 S_q)e^{\int_0^t(\lambda(s)+\mu+q)ds}. \tag{3}$$

The integration of equation (3) from 0 to $\widetilde{T}$ yields

$$S(\widetilde{T}) = e^{-\int_0^{\widetilde{T}}(\lambda(s)+\mu+q)ds}\left(S(0) + \int_0^{\widetilde{T}}(\Lambda + q_1 S_q(t))e^{\int_0^t(\lambda(s)+\mu+q)ds}dt\right) > 0.$$

Similarly, we can prove that $S(\widetilde{T}) > 0$, $S_q(\widetilde{T}) > 0$, $E(\widetilde{T}) > 0$, $I_1(\widetilde{T}) > 0$, $I_2(\widetilde{T}) > 0$, $H(\widetilde{T}) > 0$, $R(\widetilde{T}) > 0$ and $V(\widetilde{T}) > 0$.This is a contradiction to the previous claim that $S(\widetilde{T}) = 0$, $S_q(\widetilde{T}) = 0$, $E(\widetilde{T}) = 0$, $I_1(\widetilde{T}) = 0$, $I_2(\widetilde{T}) = 0$, $H(\widetilde{T}) = 0$, $R(\widetilde{T}) = 0$ or $V(\widetilde{T}) = 0$, if $\widetilde{T} < T$. Then, $\widetilde{T} = T$ and consequently the maximal solution $(S(t), S_q(t), E(t), I_1(t), I_2(t), H(t), R(t), V(t))$ of the Cauchy problem related with system (1) is positive. □

Therefore, the variables of the system (1) are positive for all time $t > 0$. In other terms, solutions of the system (1) with nonnegative initial conditions will stay positive for all $t > 0$.

Next, we consider the invariant region of the model problem (1).

Theorem 3.2. *The model problem* (1) *has solutions in the invariant region*

$$\Omega := \left\{(S, S_q, E, I_1, I_2, H, R, V) \in \mathbb{R}^8_+, \quad N(t) \leq \frac{\Lambda}{\mu} \quad \text{and} \quad V(t) \leq (f_1 + f_2 + f_3)\frac{\Lambda}{\mu d_v}\right\}.$$

Proof. We first split model system (1) into two parts i.e. the human population $(S, S_q, E, I_1, I_2, H, R)$ and the viral spread in the environment V. Then, using model system (1), the dynamics of the total human population satisfy

$$\frac{dN}{dt} = \Lambda - \mu N - d(I_1 + I_2 + H) \leq \Lambda - \mu N. \tag{4}$$

Integrating the expression above, we deduce that

$$N(t) \le \frac{\Lambda}{\mu} + \left(N(0) - \frac{\Lambda}{\mu}\right)e^{-\mu t}, \quad \forall t \ge 0,$$

where $N(0)$ is the value of $N(t)$ at the beginning. We deduce that if $N(0) \le \frac{\Lambda}{\mu}$, then $0 \le N(t) \le \frac{\Lambda}{\mu}$, $\forall t \ge 0$. Now using the fact that $I_1(t) \le \Lambda/\mu$, $I_2(t) \le \Lambda/\mu$, $E(t) \le \Lambda/\mu$, the dynamics of the viral spread in the environment satisfy

$$\frac{dV}{dt} \le (f_1 + f_2 + f_3)\frac{\Lambda}{\mu} - d_v V.$$

Integrating the expression above, we deduce that

$$V(t) \le (f_1 + f_2 + f_3)\frac{\Lambda}{\mu d_v} + \left(V(0) - (f_1 + f_2 + f_3)\frac{\Lambda}{\mu d_v}\right)e^{-d_v t}, \quad \forall t \ge 0,$$

where $V(0)$ is the initial condition of V(t). Thus, as $t \to +\infty$ we have

$$V(t) \le (f_1 + f_2 + f_3)\frac{\Lambda}{\mu d_v}.$$

Thus the region Ω is positively invariant and attracting for the system (1). It is therefore sufficient to consider the dynamics of the flow generated by the system (1). Since each maximal solution of the Cauchy problem associated with (1) is positive and bounded, each solution of the model problem (1) is global [23]. □

4 Disease-free equilibrium and its stability

For the analysis of the spread of an infection, the disease-free equilibrium (DFE) exhibits a state in the population where the disease is not prevalent and thus it is very crucial. The disease-free equilibrium is deduced from the resolution of the system of equations in (1) by taking $E = 0$, $I_1 = 0$, $I_2 = 0$, $H = 0$ and $V = 0$. Thus, the disease-free equilibrium for model (1) satisfies the system following of equations:

$$\begin{cases} (\mu + q)S^0 - q_1 S_q^0 = \Lambda, \\ qS^0 - (\mu + q_1)S_q^0 = 0. \end{cases} \tag{5}$$

Solving the system of equations in 5 yields the disease-free equilibrium point:

$$Q^0 = (S^0, S_q^0, 0, 0, 0, 0, 0),$$

where $S^0 = \frac{\Lambda(\mu + q_1)}{\mu(\mu + q + q_1)}$, $S_q^0 = \frac{\Lambda q}{\mu(\mu + q + q_1)}$ and $S^0 + S_q^0 = \frac{\Lambda}{\mu}$.

The linear stability of Q^0 depends on the basic reproductive number $\mathcal{R}_0$, which is defined as the average number of secondary cases caused by an infected individual during his/her infectivity period when he/she is introduced to a population of susceptible individuals without any intervention. We study the stability of the equilibrium through the next generation operator [24, 25]. Recalling the notations in [25] for model (1), the matrices $\mathcal{F}$ of the new infection and $\mathcal{W}$ of the remaining transfer terms are given by

$$\mathcal{F} = \begin{bmatrix} (\beta_e E + \beta_{i_1} I_1 + \beta_{i_2} I_2 + \beta_v V)S \\ 0 \\ 0 \\ 0 \\ 0 \end{bmatrix} \quad \text{and} \quad \mathcal{W} = \begin{bmatrix} \omega E + \mu E \\ -\phi\omega E + \gamma_1 I_1 + \mu I_1 + dI_1 \\ -(1-\phi)\omega E + \gamma_2 I_2 + \mu I_2 + dI_2 \\ -\gamma_1 I_1 - \gamma_2 I_2 + mH + \mu H + dH \\ -f_1 E - f_2 I_1 - f_3 I_2 + d_v V \end{bmatrix}.$$

The Jacobian matrices of $\mathcal{F}$ and $\mathcal{W}$ at Q^0 are respectively,

$$F = \begin{bmatrix} \beta_e S^0 & \beta_{i_1} S^0 & \beta_{i_2} S^0 & 0 & \beta_v S^0 \\ 0 & 0 & 0 & 0 & 0 \\ 0 & 0 & 0 & 0 & 0 \\ 0 & 0 & 0 & 0 & 0 \\ 0 & 0 & 0 & 0 & 0 \end{bmatrix} \tag{6}$$

and

$$W = \begin{bmatrix} \mu+\omega & 0 & 0 & 0 & 0 \\ -\phi\omega & \mu+\gamma_1+d & 0 & 0 & 0 \\ -(1-\phi)\omega & 0 & \mu+\gamma_2+d & 0 & 0 \\ 0 & -\gamma_1 & -\gamma_2 & \mu+m+d & 0 \\ -f_1 & -f_2 & -f_3 & 0 & d_v \end{bmatrix} \tag{7}$$

Then, the basic reproduction number of model system (1) is

$$\mathcal{R}_0 = \rho(FW^{-1}) = \mathcal{R}_{0e} + \mathcal{R}_{0i_1} + \mathcal{R}_{0i_2} + \mathcal{R}_{0v}, \tag{8}$$

where $\mathcal{R}_{0e} = \dfrac{\beta_e S^0}{\mu+\omega}$, $\mathcal{R}_{0i_1} = \dfrac{\beta_{i_1}\phi\omega S^0}{(\mu+\omega)(\mu+\gamma_1+d)}$, $\mathcal{R}_{0i_2} = \dfrac{\beta_{i_2}(1-\phi)\omega S^0}{(\mu+\omega)(\mu+\gamma_2+d)}$,

$\mathcal{R}_{0v} = \dfrac{\beta_v f_3(1-\phi)\omega(\mu+\gamma_1+d)S^0 + \beta_v(\mu+\gamma_2+d)[f_1(\mu+\gamma_1+d)+f_2\phi\omega]S^0}{d_v(\mu+\omega)(\mu+\gamma_1+d)(\mu+\gamma_2+d)}$ and $\rho(FW^{-1})$ is the spectral radius of FW^{-1}.

The term $\mathcal{R}_{0e}$ represents the average number of secondary cases caused by one exposed during its infectious period. Then the term $\mathcal{R}_{0i_1}$ (respectively $\mathcal{R}_{0i_2}$) represents the average number of secondary cases caused by one infectious timely diagnosis (respectively infectious with delayed diagnosis) during its infectious period. Similarly, the term $\mathcal{R}_{0v}$ represents the average number of secondary cases caused by one virus in the environment during its infectious period.

The importance of the basic reproduction number is due to the result given in the next Lemma established from Theorem 2 in [25].

Lemma 4.1. *The DFE Q^0 of the system* (1) *is locally asymptotically stable whenever $\mathcal{R}_0 \leq 1$ and unstable whenever $\mathcal{R}_0 > 1$.*

The biological meaning of Lemma 4.1 is that a sufficiently small number of contaminated hosts will not induce an epidemic unless $\mathcal{R}_0 > 1$. Global asymptotic stability (GAS) of the DFE is required to better control the disease. In addition , the expansion of the basin of attraction of Q^0 is a more challenging task for the model under consideration, involving a fairly new result. For this purpose, we will use Theorems 2.1 and 2.2 of [26].

Theorem 4.2. *If $\mathcal{R}_0 \leq 1$, the DFE Q^0 of the system* (1) *is GAS in Ω. If $\mathcal{R}_0 > 1$, Q^0 is unstable, the system* (1) *is uniformly persistent and there exists at least one endemic equilibrium in the interior of Ω.*

Proof. The system (1) can be written as

$$\begin{aligned} \frac{dx}{dt} &= (F-W)x - f(x,y), \\ \frac{dy}{dt} &= g(x,y), \end{aligned} \tag{9}$$

where $x = (E, I_1, I_2, H, V)^T$ is the vector representing the infected classes, $y = (S, S_q, R)^T$ is the vector representing the uninfected classes, the matrices F and W are given as in (6) and (7) respectively, and

$$f(x,y) = \begin{bmatrix} \beta_e E(S^0-S) + \beta_{i_1} I_1(S^0-S) + \beta_{i_2} I_2(S^0-S) + \beta_v V(S^0-S) \\ 0 \\ 0 \\ 0 \\ 0 \end{bmatrix}$$

and

$$g(x,y) = \begin{bmatrix} \Lambda - (\beta_e E + \beta_{i_1} I_1 + \beta_{i_2} I_2 + \beta_v V)S + q_1 S_q - (\mu + q)S \\ qS - q_1 S_q - \mu S_q \\ (\beta_e E + \beta_{i_1} I_1 + \beta_{i_2} I_2 + \beta_v V)S - \omega E - \mu E \end{bmatrix}.$$

Then,

$$W^{-1}F = \begin{bmatrix} A\beta_e S^0 & A\beta_{i_1} S^0 & A\beta_{i_2} S^0 & 0 & A\beta_v S^0 \\ B\beta_e S^0 & B\beta_{i_1} S^0 & B\beta_{i_2} S^0 & 0 & B\beta_v S^0 \\ C\beta_e S^0 & C\beta_{i_1} S^0 & C\beta_{i_2} S^0 & 0 & C\beta_v S^0 \\ D\beta_e S^0 & D\beta_{i_1} S^0 & D\beta_{i_2} S^0 & 0 & D\beta_v S^0 \\ E\beta_e S^0 & E\beta_{i_1} S^0 & E\beta_{i_2} S^0 & 0 & E\beta_v S^0 \end{bmatrix},$$

where

$$A = \frac{1}{\mu + \omega}, \quad B = \frac{\phi\omega}{(\mu + \omega)(\mu + \gamma_1 + d)} \quad C = \frac{(1-\phi)\omega}{(\mu + \omega)(\mu + \gamma_2 + d)},$$
$$D = \frac{\omega[\gamma_1\phi(\mu + \gamma_2 + d) + \gamma_2(1-\phi)(\mu + \gamma_1 + d)]}{(\mu + \omega)(\mu + \gamma_1 + d)(\mu + \gamma_2 + d)(\mu + m + d)}, \quad \text{and}$$
$$E = \frac{f_3(1-\phi)\omega(\mu + \gamma_1 + d) + (\mu + \gamma_2 + d)[f_1(\mu + \gamma_1 + d) + f_2\phi\omega]}{d_v(\mu + \omega)(\mu + \gamma_1 + d)(\mu + \gamma_2 + d)}.$$

Let $(\omega_1, \omega_2, \omega_3, \omega_4, \omega_5)$ be the left eigenvalue of $W^{-1}F$ and be given by

$$\omega_1 = \frac{\beta_e}{\beta_{i_1}}, \quad \omega_2 = 1, \quad \omega_3 = \frac{\beta_{i_1}}{\beta_v}, \quad \omega_4 = 0 \quad \text{and} \quad \omega_5 = 1, \tag{10}$$

since $(\omega_1, \omega_2, \omega_3, \omega_4, \omega_5)W^{-1}F = \mathcal{R}_0(\omega_1, \omega_2, \omega_3, \omega_4, \omega_5)$. We consider the following Lyapunov function

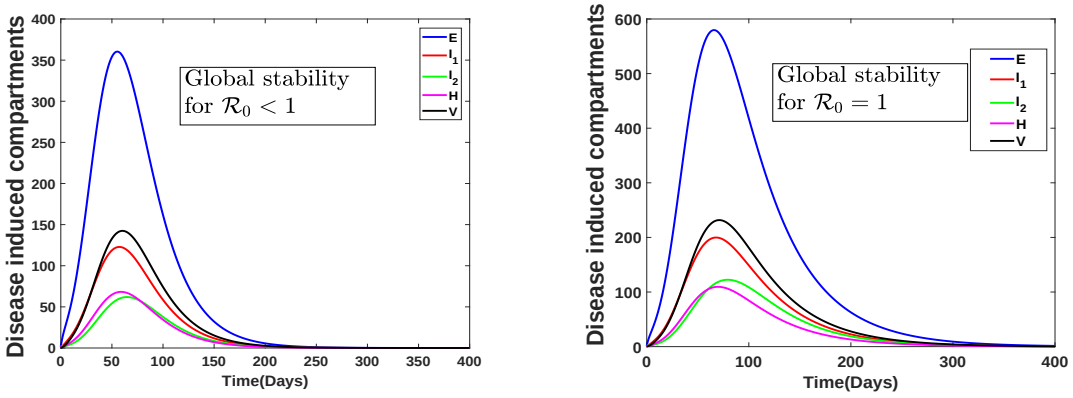

(a) (b)

Figure 3: 3(a): Global stability when $\mathcal{R}_0 < 1$, 3(b): Global stability when $\mathcal{R}_0 = 1$, in accordance with Theorem 4.2. Parameter values used are as given in Table 2, except $\gamma_2 = 1/10$, so that $\mathcal{R}_0 = 0.77 < 1$ and $\phi = 0.909$, so that $\mathcal{R}_0 = 0.95 \approx 1$.

$$Q = (\omega_1, \omega_2, \omega_3, \omega_4, \omega_5)W^{-1}(E, I_1, I_2, H, V)^T = \mathcal{A}E + \mathcal{B}I_1 + \mathcal{C}I_2 + \mathcal{D}V, \tag{11}$$

where $\mathcal{A} = \frac{\mathcal{R}_{0e}}{\beta_{i_1}S^0} + \frac{\mathcal{R}_{0i_1}}{\beta_{i_1}S^0} + \frac{\mathcal{R}_{0i_2}}{\beta_v S^0} + \frac{\mathcal{R}_{0v}}{\beta_v S^0}$, $\mathcal{B} = \frac{d_v + f_2}{d_v(\mu + \gamma_1 + d)}$, $\mathcal{C} = \frac{\beta_{i_2}d_v + f_3\beta_v}{\beta_v d_v(\mu + \gamma_2 + d)}$ and $\mathcal{D} = \frac{1}{d_v}$. Then the derivative of the Lyapunov function Q yields,

$$Q' = (\mathcal{R}_0 - 1)(\omega_1, \omega_2, \omega_3, \omega_4, \omega_5)^T x - (\omega_1, \omega_2, \omega_3, \omega_4, \omega_5)^T W^{-1} f(x, y).$$

Since $(\omega_1, \omega_2, \omega_3, \omega_4, \omega_5) \geq 0$, $W^{-1} \geq 0$ and $f(x, y) \geq 0$ in Ω, then $(\omega_1, \omega_2)^T W^{-1} f(x, y) \geq 0$. Therefore, $Q^{'} \leq 0$ in Ω if $\mathcal{R}_0 \leq 1$ and Q is a Lyapunov function for the system (1). By LaSalle's invariance principle [27, 28], Q^0 is GAS in Ω [13].

If $\mathcal{R}_0 > 1$, then $Q^{'} = (\mathcal{R}_0 - 1)(\omega_1, \omega_2, \omega_3, \omega_4, \omega_5)^T x > 0$ provided that $x > 0$ and $y = (S^0, S_q^0, 0)$. By continuity, $Q^{'} > 0$ in the neighborhood of Q^0. Solutions in positive cone sufficiently close to Q^0 move away from Q^0, implying that Q^0 is unstable. Thus, the model system (1) is uniformly persistent [29, 30]. Uniform persistence and the positively invariance of Ω imply the existence of an endemic equilibrium. □

As a consequence of this result above, we can confidently deduce that COVID-19 can be eradicated from the host community if the value of $\mathcal{R}_0$ can be reduced and retained less than the unity. Figure 3 shows the validation of the global stability analysis for the disease-free equilibrium point.

5 Endemic equilibrium and its stability

Let $Q^* = (S^*, S_q^*, I_1^*, I_2^*, H^*, R^*, V^*)$ be the positive endemic equilibrium (EE) of model system (1). Then, the positive endemic equilibrium can be obtained by setting the right hand side of all equations in model system (1) to zero, giving:

$$\begin{cases} \Lambda - \lambda^* S^* + q_1 S_q^* - (\mu + q) S^* & = 0, \\ q S^* - q_1 S_q^* - \mu S_q^* & = 0, \\ \lambda^* S^* - \omega E^* - \mu E^* & = 0, \\ \phi\omega E^* - \gamma_1 I_1^* - \mu I_1^* - d I_1^* & = 0, \\ (1-\phi)\omega E^* - \gamma_2 I_2^* - \mu I_2^* - d I_2^* & = 0, \\ \gamma_1 I_1^* + \gamma_2 I_2^* - m H^* - \mu H^* - d H^* & = 0, \\ m H^* - \mu R^* & = 0, \\ f_1 E^* + f_2 I_1^* + f_3 I_2^* - d_v V^* & = 0, \end{cases} \tag{12}$$

where $\lambda^* = \beta_e E^* + \beta_{i_1} I_1^* + \beta_{i_2} I_2^* + \beta_v V^*$. Given the complexity of the system (12), we are going to try to determine an explicit formula for the endemic equilibrium point Q^*. To do this, we will solve the system (12). After algebraic manipulations of this system, we obtain:

$$\begin{aligned} R^* &= \frac{m}{\mu} H^*, E^* = \frac{\mu + \gamma_1 + d}{\phi\omega} I_1^*, I_2^* = \frac{(1-\phi)(\mu + \gamma_1 + d)}{\phi(\mu + \gamma_2 + d)} I_1^*, S_q^* = \frac{q_1 + \mu}{q} S^*, \\ H^* &= \frac{\gamma_1 \phi(\mu + \gamma_2 + d) + \gamma_2(1-\phi)(\mu + \gamma_1 + d)}{\phi(\mu + \gamma_2 + d)(\mu + m + d)} I_1^*, \\ V^* &= \frac{f_1(\mu + \gamma_1 + d)(\mu + \gamma_2 + d) + f_2\phi\omega(\mu + \gamma_2 + d) + f_3(1-\phi)\omega(\mu + \gamma_1 + d)}{\phi\omega d_v(\mu + \gamma_2 + d)} I_1^*, \\ S^* &= \frac{d_v(\mu + \omega)(\mu + \gamma_1 + d)(\mu + \gamma_2 + d)}{\beta_e d_v(\mu + \gamma_1 + d)(\mu + \gamma_2 + d) + \beta_{i_1}\phi\omega d_v(\mu + \gamma_2 + d) + \beta_{i_2}(1-\phi)\omega d_v(\mu + \gamma_1 + d)} \\ &\quad + \frac{d_v(\mu + \omega)(\mu + \gamma_1 + d)(\mu + \gamma_2 + d)}{\beta_v f_1(\mu + \gamma_1 + d)(\mu + \gamma_2 + d) + \beta_v f_2\phi\omega(\mu + \gamma_2 + d) + \beta_v f_3(1-\phi)\omega(\mu + \gamma_1 + d)}, \end{aligned}$$

and

$$I_1^* = \frac{\phi\omega[(q + \mu)(q_1 + \mu) - q q_1]}{(q_1 + \mu)(\mu + \omega)(\mu + \gamma_1 + d)} S^*(\mathcal{R}_0 - 1).$$

Lemma 5.1. *Model* (1) *has exactly one endemic equilibrium whenever* $\mathcal{R}_0 > 1$.

We establish the following result to analyze the stability of Q^* by using the Lyapunov function of Goh-Volterra type, see, e.g. [26, 31, 32, 34].

Theorem 5.2. *If* $\mathcal{R}_0 > 1$, *the endemic equilibrium* Q^* *is GAS in* Ω.

Proof. Consider the following Lyapunov function candidate:

$$L = \left(S - S^\star - S^\star \ln \frac{S}{S^\star}\right) + h_1\left(S_q - S_q^\star - S_q^\star \ln \frac{S_q}{S_q^\star}\right) + h_2\left(E - E^\star - E^\star \ln \frac{E}{E^\star}\right) + h_3\left(I_1 - I_1^\star - I_1^\star \ln \frac{I_1}{I_1^\star}\right) + h_4\left(I_2 - I_2^\star - I_2^\star \ln \frac{I_2}{I_2^\star}\right) + h_5\left(V - V^\star - V^\star \ln \frac{V}{V^\star}\right), \tag{13}$$

where h_1, h_2, h_3, h_4 and h_5 are positive constants to be determined later. Differentiating the function (13) with respect to time yields

$$\dot{L} = \left(1 - \frac{S^\star}{S}\right)\dot{S} + h_1\left(1 - \frac{S_q^\star}{S_q}\right)\dot{S}_q + h_2\left(1 - \frac{E^\star}{E}\right)\dot{E} + h_3\left(1 - \frac{I_1^\star}{I_1}\right)\dot{I}_1 + h_4\left(1 - \frac{I_2^\star}{I_2}\right)\dot{I}_2 + h_5\left(1 - \frac{V^\star}{V}\right)\dot{V}. \tag{14}$$

Substituting equation (1) into equation (14) and using Equation (12) at the positive endemic equilibrium with further simplification yields

$$\begin{aligned}
\dot{L} =& -(q_1+\mu)\left(1-\frac{1}{x_1}\right)^2 S + \beta_e S^\star E^\star\left(1 - \frac{1}{x_1} + x_3 - x_1x_3\right) + \beta_{i_1} S^\star I_1^\star\left(1 - \frac{1}{x_1} + x_4 - x_1x_4\right) \\
&+ \beta_{i_2} S^\star I_2^\star\left(1 - \frac{1}{x_1} + x_5 - x_1x_5\right) + \beta_v S^\star V^\star\left(1 - \frac{1}{x_1} + x_6 - x_1x_6\right) + q_1 S_q^\star\left(x_2 + \frac{1}{x_1} - \frac{x_2}{x_1} - 1\right) \\
&+ h_1 q S^\star\left(x_1 - x_2 - \frac{x_1}{x_2} + 1\right) + h_2\beta_e S^\star E^\star\left(1 - x_1 - x_3 + x_1x_3\right) + h_2\beta_{i_1} S^\star I_1^\star\left(1 - x_3 + x_1x_4 - \frac{x_1x_4}{x_3}\right) \\
&+ h_2\beta_{i_2} S^\star I_2^\star\left(1 - x_3 + x_1x_5 - \frac{x_1x_5}{x_3}\right) + h_2\beta_v S^\star V^\star\left(1 - x_3 + x_1x_6 - \frac{x_1x_6}{x_3}\right) \\
&+ h_3\phi\omega E^\star\left(1 + x_3 - x_4 - \frac{x_3}{x_4}\right) + h_4(1-\phi)\omega E^\star\left(1 + x_3 - x_5 - \frac{x_3}{x_5}\right) + h_5 f_1 E^\star\left(1 + x_3 - x_6 - \frac{x_3}{x_6}\right) \\
&+ h_5 f_2 I_1^\star\left(1 + x_4 - x_6 - \frac{x_4}{x_6}\right) + h_5 f_3 I_2^\star\left(1 + x_5 - x_6 - \frac{x_5}{x_6}\right),
\end{aligned} \tag{15}$$

where $x_1 = \frac{S}{S^\star}$, $x_2 = \frac{S_q}{S_q^\star}$, $x_3 = \frac{E}{E^\star}$, $x_4 = \frac{I_1}{I_1^\star}$, $x_5 = \frac{I_2}{I_2^\star}$ and $x_6 = \frac{V}{V^\star}$. Then equation (15) becomes

$$\begin{aligned}
\dot{L} =& -(q_1+\mu)\left(1-\frac{1}{x_1}\right)^2 S + \beta_e S^\star E^\star + \beta_{i_1} S^\star I_1^\star + \beta_{i_2} S^\star I_2^\star + \beta_v S^\star V^\star - q_1 S_q^\star + h_1 q S^\star \\
&+ h_2\beta_e S^\star E^\star + h_2\beta_{i_1} S^\star I_1^\star + h_2\beta_{i_2} S^\star I_2^\star + h_2\beta_v S^\star V^\star + h_3\phi\omega E^\star + h_4(1-\phi)\omega E^\star + h_5 f_1 E^\star \\
&+ h_5 f_2 I_1^\star + h_5 f_3 I_2^\star + \left(-\beta_e S^\star E^\star - \beta_{i_1} S^\star I_1^\star - \beta_{i_2} S^\star I_2^\star - \beta_v S^\star V^\star + q_1 S_q^\star\right)\frac{1}{x_1} \\
&+ (h_1 q S^\star - h_2\beta_e S^\star E^\star)x_1 + (q_1 S_q^\star - h_1 q S^\star)x_2 + (\beta_e S^\star E^\star - h_2\beta_e S^\star E^\star - h_2\beta_{i_1} S^\star I_1^\star \\
&- h_2\beta_{i_2} S^\star I_2^\star - h_2\beta_v S^\star V^\star + h_3\phi\omega E^\star + h_4(1-\phi)\omega E^\star + h_5 f_1 E^\star)x_3 \\
&+ (\beta_{i_1} S^\star I_1^\star - h_3\phi\omega E^\star + h_5 f_2 I_1^\star)x_4 + (\beta_{i_2} S^\star I_2^\star + h_4(1-\phi)\omega E^\star + h_5 f_3 I_2^\star)x_5 \\
&+ (\beta_v S^\star V^\star - h_5 f_1 E^\star - h_5 f_2 I_1^\star - h_5 f_3 I_2^\star)x_6 + (-\beta_e S^\star E^\star + h_2\beta_e S^\star E^\star)x_1x_3 \\
&+ (-\beta_{i_1} S^\star I_1^\star + h_2\beta_{i_1} S^\star I_1^\star)x_1x_4 + (-\beta_{i_2} S^\star I_2^\star + h_2\beta_{i_2} S^\star I_2^\star)x_1x_5 \\
&+ (-\beta_v S^\star V^\star + h_2\beta_v S^\star V^\star)x_1x_6 - q_1 S_q^\star\frac{x_2}{x_1} + h_1 q S^\star\frac{x_1}{x_2} - h_3\phi\omega E^\star\frac{x_3}{x_4} - h_4(1-\phi)\omega E^\star\frac{x_3}{x_5} \\
&- h_5 f_1 E^\star\frac{x_3}{x_6} - h_5 f_2 I_1^\star\frac{x_4}{x_6} - h_5 f_3 I_2^\star\frac{x_5}{x_6} - h_2\beta_{i_1} S^\star I_1^\star\frac{x_1x_4}{x_3} - h_2\beta_{i_2} S^\star I_2^\star\frac{x_1x_5}{x_3} - h_2\beta_v S^\star V^\star\frac{x_1x_6}{x_3}.
\end{aligned} \tag{16}$$

Considering the expressions

$$h_2\beta_e S^\star E^\star = \beta_e S^\star E^\star,\ h_2\beta_{i_1} S^\star I_1^\star = \beta_{i_1} S^\star I_1^\star, h_2\beta_{i_2} S^\star I_2^\star = \beta_{i_2} S^\star I_2^\star,\ \text{and}\ h_2\beta_v S^\star V^\star = \beta_v S^\star V^\star,$$

we have $h_2 = 1$, thus the coefficients of x_1x_3, x_1x_4, x_1x_5 and x_1x_6 are all 0. By setting the coefficients of x_2, x_3, x_4, x_5, and x_6 to 0 and solving for h_1, h_3, h_4 and h_5 yields

$$h_1 = \frac{q_1 S_q^\star}{q S^\star}, \quad h_3 = \frac{\beta_{i_1} S^\star I_1^\star(f_1 E^\star + f_2 I_1^\star + f_3 I_2^\star) + \beta_v f_2 S^\star V^\star I_1^\star}{\phi\omega E^\star(f_1 E^\star + f_2 I_1^\star + f_3 I_2^\star)},$$

$$h_4 = \frac{\beta_{i_2} S^\star I_2^\star (f_1 E^\star + f_2 I_1^\star + f_3 I_2^\star) + \beta_v f_3 S^\star V^\star I_1^\star}{(1-\phi)\omega E^\star (f_1 E^\star + f_2 I_1^\star + f_3 I_2^\star)} \quad \text{and} \quad h_5 = \frac{\beta_v S^\star V^\star}{f_1 E^\star + f_2 I_1^\star + f_3 I_2^\star}.$$

Therefore, $\dot{L}$ can be rewritten as

$$\begin{aligned}
\dot{L} = &-(q_1+\mu)\left(1-\frac{1}{x_1}\right)^2 S - \beta_e S^\star E^\star \left(x_1 + \frac{1}{x_1} - 2\right) \\
&- \beta_{i_1} S^\star I_1^\star \left(x_3 - x_4 + \frac{1}{x_1} + \frac{x_1 x_4}{x_3} - 2\right) - \beta_{i_2} S^\star I_2^\star \left(x_3 - x_5 + \frac{1}{x_1} + \frac{x_1 x_5}{x_3} - 2\right) \\
&- \beta_v S^\star V^\star \left(x_3 - x_6 + \frac{1}{x_1} + \frac{x_1 x_6}{x_3} - 2\right) - q_1 S_q^\star \left(\frac{x_1}{x_2} + \frac{x_2}{x_1} - x_1 - \frac{1}{x_1}\right) \\
&- h_3 \phi \omega E^\star \left(x_4 - x_3 - 1 + \frac{x_3}{x_4}\right) - h_4 (1-\phi)\omega E^\star \left(x_5 - x_3 - 1 + \frac{x_3}{x_5}\right) \\
&- h_5 f_1 E^\star \left(x_6 - x_3 - 1 + \frac{x_3}{x_6}\right) - h_5 f_2 I_1^\star \left(x_6 - x_4 - 1 + \frac{x_4}{x_6}\right) - h_5 f_3 I_2^\star \left(x_6 - x_5 - 1 + \frac{x_5}{x_6}\right).
\end{aligned}$$

Thus, using the arithmetic-geometric means inequality, we can see that $\dot{L}$ is less or equal to zero with equality only if $x_1 = 1$, $x_2 = 1$, $x_2 = 1$, $x_3 = 1$, $x_4 = 1$, $x_5 = 1$ and $x_6 = 1$. By LaSalle's invariance principle the largest invariant set in Ω, contained in

$$\{(S, S_q, E, I_1, I_2, H, R, V) \in \Omega \quad | \quad \dot{L} = 0\}$$

is reduced to the endemic equilibrium $Q^\star$. Then, we conclude that the endemic equilibrium is globally asymptotically stable in Ω [33, 34]. □

Figure 4 shows the validation of the global stability analysis for the endemic equilibrium point.

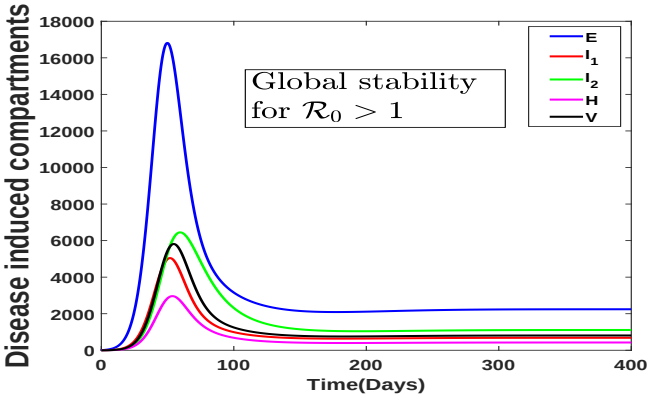

Figure 4: Global stability when $\mathcal{R}_0 > 1$, in accordance with Theorem 5.2. Parameter values used are as given in Table 2, except $\phi = 0.8$, so that $\mathcal{R}_0 = 2.06 > 1$.

6 Numerical Results

In this section, we present numerical simulations of the proposed model (1) using parameter estimated from COVID-19 data for Ghana [35]. The estimation was done by using the least squares approach which consists of minimizing the sum of the squared differences between each observed cummulative case data point and the corresponding cummulative cases point obtained from the model (1), i.e. $\sum_{i=1}^{N}(y_i - y_d)^2$, where y_i is the solution to the model with a set of estimated parameters and y_d is the reported data, see, e.g. [36]. In Figure 5, we present the fitted model, the cumulative cases and residual plot for Ghana using 100 data points. The

initial conditions are taken on the date of the first confirmed cases i.e. 12th March, 2020. The incubation periods of COVID-19 is known to be 2 – 14 days. On 12th March, 2020, the first two COVID-19 cases were reported in Ghana, hence, we took the initial hospitalized to be two i.e. $H(0) = 2$, the total population of Ghana was $30,417,856$. It is assumed that, there were no recoveries, but equal number of exposed, timely, and delayed people as the first two detected cases during the initial stages. Therefore, the initial values for Ghana are given by $S(0) = 30417848, S_q(0) = 0, E(0) = 2, I_1(0) = 2\ I_2(0) = 2\ H(0) = 2\ R(0) = 0\ V(0) = 0$. From the data fitting, as shown in Figure 5 and Table 2, the computed reproduction number, $\mathcal{R}_0$, for the 100 data points is given as $\mathcal{R}_c = 1.0410$. In what follows, we show the sensitivity analysis and other numerical outputs of the model using the obtained parameters in Table 1.

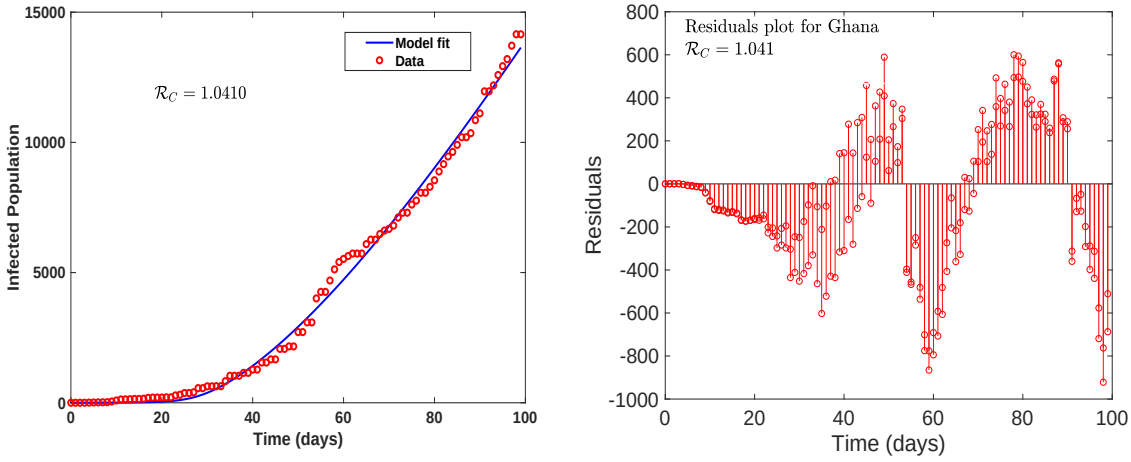

(a) Model fit

(b) Residual plot.

Figure 5: Model fit for Ghana during the time window 12 March, 2020 to 19 June, 2020 .

Table 2: Estimated parameters .

Parameters	Value/day	Source	Parameters	Value/day	Source
Λ	1319.294	[37]	γ_1	0.5000	Fitted
q	0.0333	Fitted	γ_2	0.0714	Fitted
q_1	1.6945×10^{-5}	Estimated	μ	4.2578×10^{-5}	[38]
β_e	6.0380×10^{-8}	Fitted	d	0.006139	Estimated
β_{i_1}	3.8196×10^{-8}	Fitted	f_1	0.0178	Fitted
β_{i_2}	1.4286×10^{-5}	Fitted	f_2	0.3115	Fitted
β_v	4.00199×10^{-8}	[13]	f_3	4.6131×10^{-5}	Fitted
ω	1/5.2	[38]	m	0.9815	Fitted
ϕ	0.9000 unitless	Fitted	d_v	0.3117	[39]

7 Global sensitivity analysis

In this section we present the graphical representation for the 18 parameters in basic reproduction number, $\mathcal{R}_0$, using scatter plots and Latin Hypercube Sampling (LHS). Scatter plots are used to obtain the correlations of the various parameters in the basic reproduction number, $\mathcal{R}_0$. They also give undeniable visual connection of the various parameters in $\mathcal{R}_0$. It can vary from −1 (perfect negative correlation) through 0 (no correlation) to +1 (perfect positive correlation). LHS is known to be a Monte Carlo sampling method. It divides the various parameters into equal even intervals and indiscriminately draws one sample from each equal interval once. LHS is usually carried out with partial rank correlation coefficient (PRCC) to estimate the nonlinearity between the parameters, and also the unmodulated, relationship between model parameters, see, e.g. [40, 41].

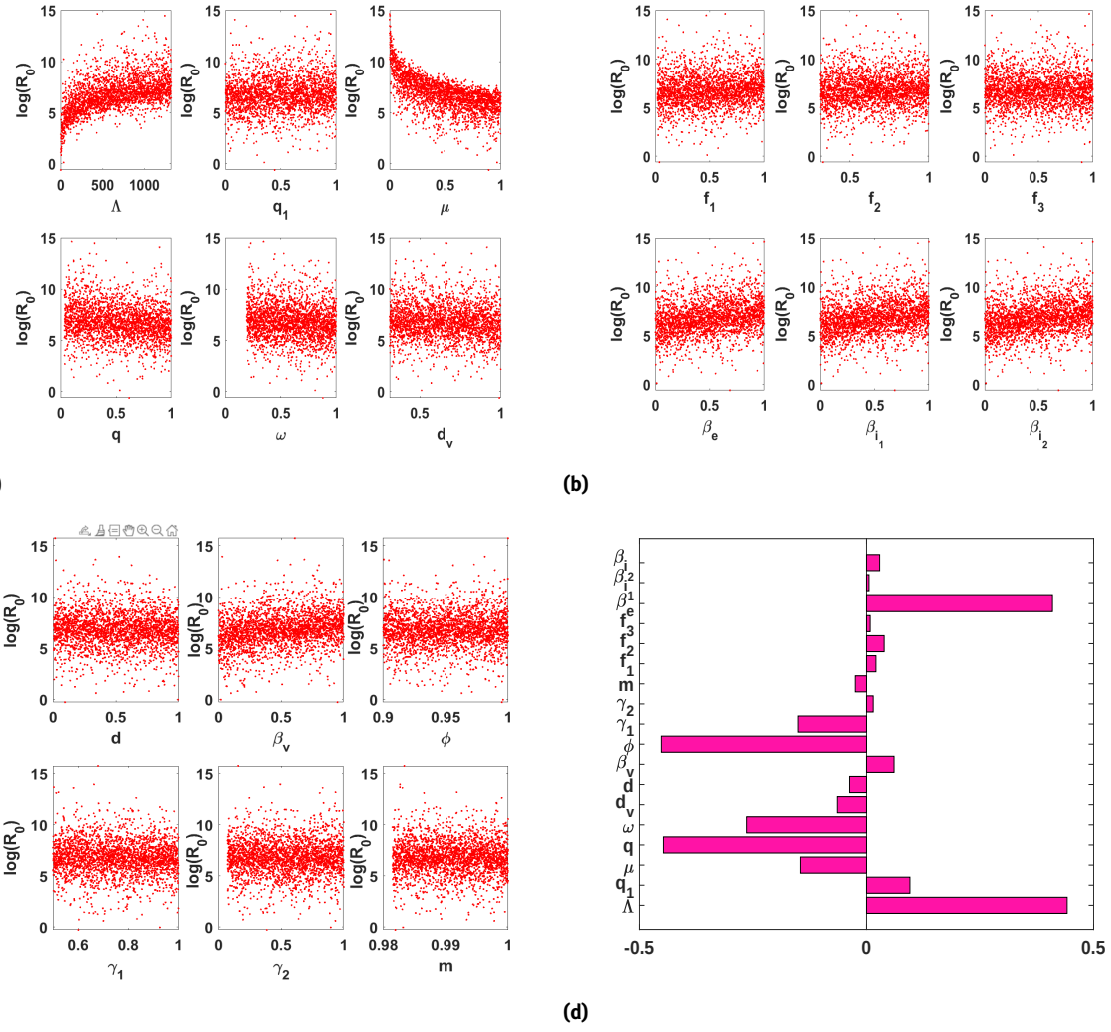

Figure 6: Global sensitivity analysis plot for COVID-19 model with timely-delayed diagnosis

Using the LHS with 2500 samples from a uniform distribution, the parameters in the basic reproduction number $\mathcal{R}_0$, were employed to obtain the global sensitivity of the various parameters in $\mathcal{R}_0$. Figures 6(a) to 6(c) depict the scatter relation of the various parameters in the basic reproduction number. Particularly, Figure 6(a) shows the relation of Λ, q_1, μ, q, ω, and d_v to the logarithmic relation of $\mathcal{R}_0$. We notice that each sample point in Λ and μ has a 100% clear direction with the basic reproduction number. Figures 6(b) and 6(c) give

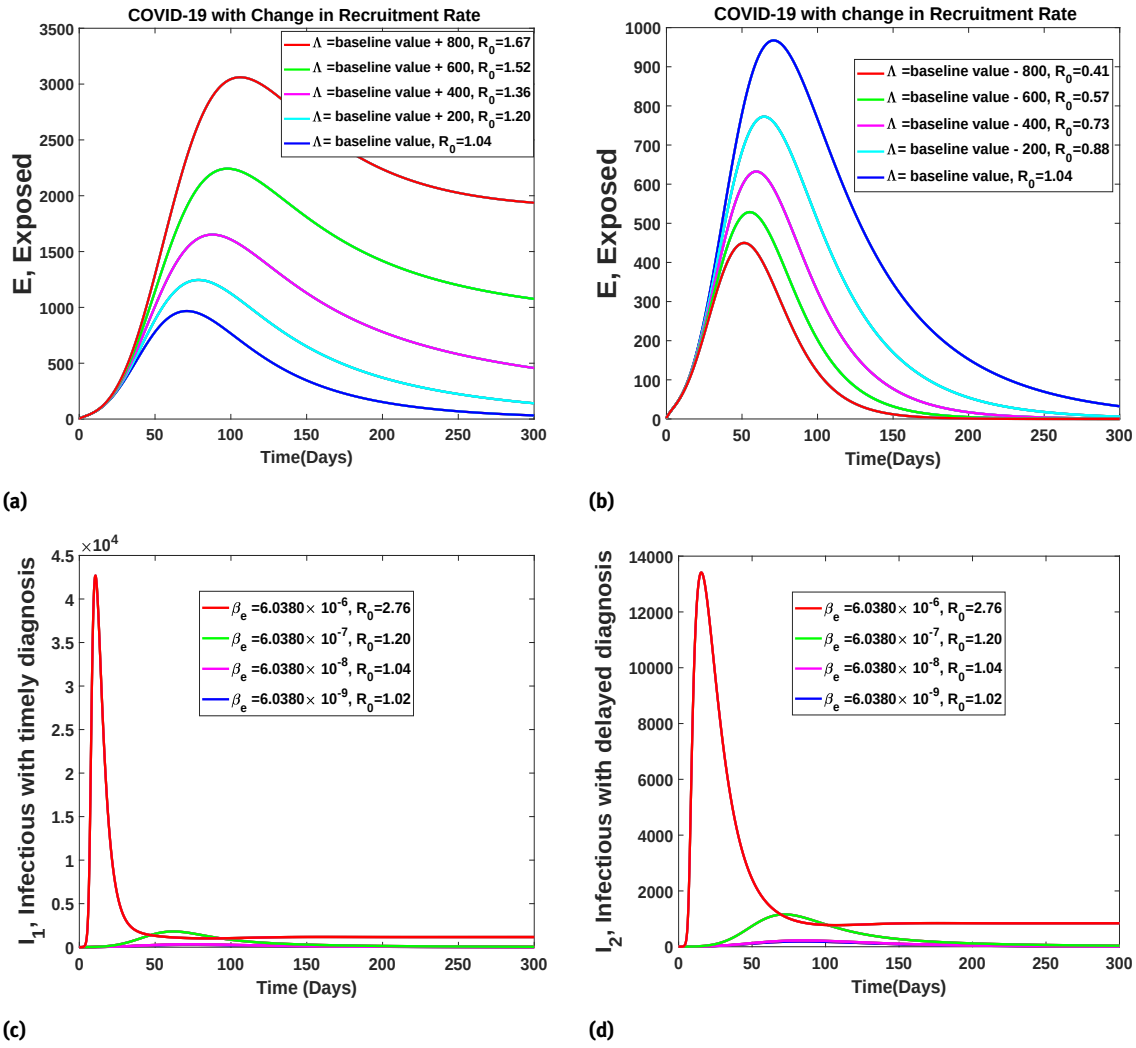

Figure 7: Sensitivity analysis plot for COVID-19 model with timely-delayed diagnosis, using Λ, and β_e.

an undetermined relation of the other parameters to $\mathcal{R}_0$. Using the PRCC plot in Figure 6(d), we noticed that the parameters contributing to the growth of the basic reproduction number are $\Lambda, \beta_e, q_1, f_2, \beta_{i_2}, f_1, \gamma_2, f_3$, and β_{i_1} (arranged in order of magnitude). While $\phi, q, \omega, \gamma_1, \mu, d_v, d$ and m contribute to the decline of the basic reproduction number, $\mathcal{R}_0$ (arranged in order of magnitude). Among the positive parameters, Λ and β_e are the most dominant parameters, hence it suggests that a reduction in the number of new inflow Λ, and the interaction of exposed individuals β_e, in the population will reduce the rate of the virus spread in the local community or the basic reproduction number faster then the other parameters. Among the negative parameters, ϕ, q, ω and γ_1 are the most dominant parameters, hence, an increase in these parameters will reduce the rate of the viral spread in the local community or the basic reproduction number faster than the other parameters, $\mu, d_v, d\ m$. Therefore, in Figures 7 and 8 we show the graphical trajectories of the parameters on the infected classes.

In Figures 7(a)to 7(d), we show the impact of the rate of recruitment Λ, and the rate of relative transmissibility of exposed individuals β_e, on the model. We noticed in Figure 7(a) that an increase in Λ, will have a direct increase in the number of new infections whiles Figure 7(b) shows that, a decline in Λ, will help eradicate the disease in Ghana. In Figures 7(c) and 7(d), we notice that an increase in the relative transmissibility of exposed individuals will have an exponential growth in the number of secondary infections. Hence, we suggest that all persons should keep to the regular washing of hands with soap and alcohol based sanitizer

whenever they use public facilities, since this will help reduce the spread of the virus by exposed individuals. In Figures 8(a) and Figure 8(b), we showed the dynamical effects of varying the proportion of the infectious with timely diagnosis and self-quarantined rate of the susceptible individuals. Figure 8(a) indicates that, an increase in the proportion of the infectious with timely diagnosis reduces the basic reproduction number and that a 100% detection of infected individuals on time will have the basic reproduction reducing to 0.025, resulting in a complete eradication of the disease within 100 days. In Figure 8(b) we noticed that the willingness of individuals to practice self-quarantine has a major role in reducing the disease spread in Ghana. In Figure 8(c) we show the dynamical effect of incubation period of the disease on the number of timely-delayed diagnosis individuals. We noticed that an increase in the number of incubation period reduce the number of timely-delayed diagnosis individuals. Figure 8(d) shows the dynamical effects of delayed diagnosis on the number of exposed individuals. The Figure 8(d) shows that, a reduction in time delayed reduces the number of exposed individuals, hence, we suggest that the government should increase their efforts in diagnoses so to reduce the number of infected individuals in each community.

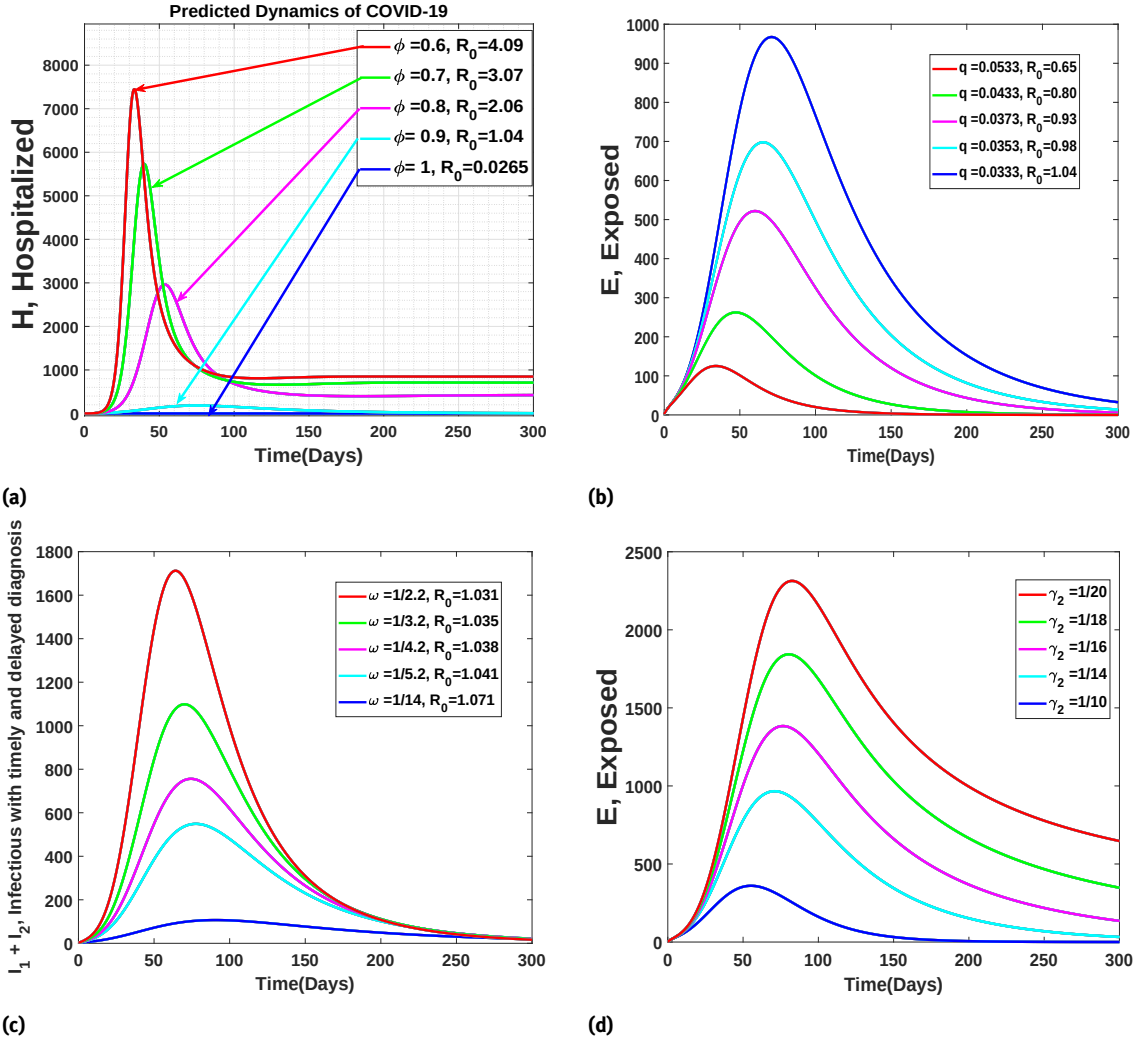

Figure 8: Sensitivity analysis plot for COVID-19 model with timely-delayed diagnosis, using ϕ, q, ω and γ_2.

8 Conclusion

In this article, we presented a COVID-19 model that considers self-quarantined individuals, delay in diagnosis and environmental transmission and analysed the transmission dynamics of the pandemic in Ghana. The proposed model was shown to be globally asymptotically stable when $\mathcal{R}_0 \leq 1$ and when $\mathcal{R}_0 > 1$. The numerical simulations of the model suggest that, the recruitment rate positively increase the number of new infections, likewise the rate of transmissibility of exposed individuals. Figure 7(c) and 7(d) shows that, an increase in the relative transmissibility of exposed individuals will have an exponential growth in the number of secondary infections. Hence, we suggest that all persons should keep to the regular washing of hands with soap and alcohol based sensitizer whenever they use public facilities, since this will help reduce the spread of the virus by exposed individuals. We also noticed from Figure 8(d) that, timely diagnosis can reduce the number of exposed individuals in Ghana, hence, we suggest that the government should increase their efforts in diagnoses so to reduce the number of infected individuals in each community.

Acknowledgements: SEM was supported by a grant from UNESCO-TWAS and the Swedish International Development Cooperation Agency (SIDA). The views expressed herein do not necessarily represent those of UNESCO-TWAS, SIDA or its Board of Governors. HLB was funded by a grant from the African Institute for Mathematical Sciences (www.nexteinstein.org), with financial support from the Government of Canada, provided through Global Affairs Canada (www.international.gc.ca), and the International Development Research Centre (www.idrc.ca).

Conflict of Interests Statement: The authors have no conflict of interest to disclose.

Ethics Statement This research did not require ethical approval.

References

[1] W. H. Organization, WHO characterizes covid-19 as a pandemic„ https://www.who.int/dg/speeches/detail/who-director-general (2020).
[2] M. Moriyama, W. J. Hugentobler, A. Iwasaki, Seasonality of respiratory viral infections, Annual review of virology 7 (2020) 83–101.
[3] W. H. Organization, WHO weekly operational update on covid-19„ https://www.who.int/docs/default-source/coronaviruse/situation-reports (2020).
[4] J. Duncan, Two cases of coronavirus confirmed in ghana, citi newsroom (Retrieved 16 March 2020).
[5] J. K. K. Asamoah, C. Bornaa, B. Seidu, Z. Jin, Mathematical analysis of the effects of controls on transmission dynamics of sars-cov-2, Alexandria Engineering Journal 59 (6) (2020) 5069–5078.
[6] S. Djaoue, G. G. Kolaye, H. Abboubakar, A. A. A. Ari, I. Damakoa, Mathematical modeling, analysis and numerical simulation of the covid-19 transmission with mitigation of control strategies used in cameroon, Chaos, Solitons & Fractals 139 (2020) 110281.
[7] M. A. Khan, A. Atangana, E. Alzahrani, et al., The dynamics of covid-19 with quarantined and isolation, Advances in Difference Equations 2020 (1) (2020) 1–22.
[8] E. Alzahrani, M. El-Dessoky, D. Baleanu, Modeling the dynamics of the novel coronavirus using caputo-fabrizio derivative, Alexandria Engineering Journal 60 (5) (2021) 4651–4662.
[9] Z. Zhang, A. Zeb, S. Hussain, E. Alzahrani, Dynamics of covid-19 mathematical model with stochastic perturbation, Advances in Difference Equations 2020 (1) (2020) 1–12.
[10] X. Rong, L. Yang, H. Chu, M. Fan, Effect of delay in diagnosis on transmission of covid-19, Math Biosci Eng 17 (3) (2020) 2725–2740.
[11] Y. Fang, Y. Nie, M. Penny, Transmission dynamics of the covid-19 outbreak and effectiveness of government interventions: A data-driven analysis, Journal of medical virology 92 (6) (2020) 645–659.
[12] F. Ndaïrou, I. Area, J. J. Nieto, D. F. Torres, Mathematical modeling of covid-19 transmission dynamics with a case study of wuhan, Chaos, Solitons & Fractals 135 (2020) 109846.
[13] J. K. K. Asamoah, M. A. Owusu, Z. Jin, F. Oduro, A. Abidemi, E. O. Gyasi, Global stability and cost-effectiveness analysis of covid-19 considering the impact of the environment: using data from ghana, Chaos, Solitons & Fractals 140 (2020) 110103.

[14] E. Acheampong, E. Okyere, S. Iddi, J. H. Bonney, J. K. K. Asamoah, J. A. Wattis, R. L. Gomes, Mathematical modelling of earlier stages of covid-19 transmission dynamics in ghana, Results in Physics 34 (2022) 105193. doi:https://doi.org/10.1016/j.rinp.2022.105193.
URL https://www.sciencedirect.com/science/article/pii/S2211379722000134
[15] S. Olaniyi, O. S. Obabiyi, K. Okosun, A. Oladipo, S. Adewale, Mathematical modelling and optimal cost-effective control of covid-19 transmission dynamics, The European Physical Journal Plus 135 (11) (2020) 938.
[16] L. Nkague Nkamba, T. T. Manga, Modelling and prediction of the spread of covid-19 in cameroon and assessing the governmental measures $march - september2020$, COVID 1 (3) (2021) 622–644. doi:10.3390/covid1030052.
URL https://www.mdpi.com/2673-8112/1/3/52
[17] W. A. Halatoko, Y. R. Konu, F. A. Gbeasor-Komlanvi, A. J. Sadio, M. K. Tchankoni, K. S. Komlanvi, M. Salou, A. M. Dorkenoo, I. Maman, A. Agbobli, M. I. Wateba, K. S. Adjoh, E. Goeh-Akue, Y.-b. Kao, I. Kpeto, R. Pana, Paul Kinde-Sossou, A. Tamekloe, J. Nayo-Apétsianyi, S.-P. H. Assane, M. Prine-David, S. M. Awoussi, M. Djibril, M. Mijiyawa, A. C. Dagnra, D. K. Ekouevi, Prevalence of sars-cov-2 among high-risk populations in lomé *togo* in 2020, PLOS ONE 15 (11) (2020) 1–12. doi:10.1371/journal.pone.0242124.
URL https://doi.org/10.1371/journal.pone.0242124
[18] C. H. Nkwayep, S. Bowong, B. Tsanou, M. A. A. Alaoui, J. Kurths, Mathematical modeling of covid-19 pandemic in the context of sub-saharan africa: a short-term forecasting in cameroon and gabon, Mathematical Medicine and Biology: A Journal of the IMA 39 (1) (2022) 1–48. arXiv:https://academic.oup.com/imammb/article-pdf/39/1/1/42576019/dqab020.pdf, doi:10.1093/imammb/dqab020.
URL https://doi.org/10.1093/imammb/dqab020
[19] S. E. Moore, E. Okyere, Controlling the transmission dynamics of covid-19, Commun. Math. Biol. Neurosci. 2020 (6).
[20] Q. Li, X. Guan, P. Wu, X. Wang, L. Zhou, Y. Tong, R. Ren, K. S. Leung, E. H. Lau, J. Y. Wong, et al., Early transmission dynamics in wuhan, china, of novel coronavirus–infected pneumonia, New England journal of medicine.
[21] S. Cheng, Y. Chen, W.and Yang, P. Chu, X. Liu, M. Zhao, W. Tan, L. Xu, Q. Wu, H. Guan, J. Liu, Effect of diagnostic and treatment delay on the risk of tuberculosis transmission in shenzhen, china: an observational cohort study, 1993–2010, PLoS One 8 (6) (2013) e67516.
[22] C. Kraef, A. Bentzon, A.and Panteleev, A. Skrahina, N. Bolokadze, S. Tetradov, R. Podlasin, I. Karpov, E. Borodulina, E. Denisova, I. Azina, Delayed diagnosis of tuberculosis in persons living with hiv in eastern europe: associated factors and effect on mortality—a multicentre prospective cohort study, BMC infectious diseases 21 (1) (2021) 1–12.
[23] A. Gumel, A. Enahoro, N. Calistus, A. Gideon, Mathematical assessment of the roles of vaccination and non-pharmaceutical interventions on covid-19 dynamics: a multigroup modeling approach, medRxiv (2021) 2020.12. 11.20247916.
[24] J. A. Jacquez, C. P. Simon, Qualitative theory of compartmental systems, Siam Review 35 (1) (1993) 43–79.
[25] P. Van den Driessche, J. Watmough, Reproduction numbers and sub-threshold endemic equilibria for compartmental models of disease transmission, Mathematical biosciences 180 (1-2) (2002) 29–48.
[26] Z. Shuai, P. van den Driessche, Global stability of infectious disease models using lyapunov functions, SIAM Journal on Applied Mathematics 73 (4) (2013) 1513–1532.
[27] J. P. La Salle, The stability of dynamical systems, SIAM, 1976.
[28] J. La Salle, S. Lefschetz, Stability by Liapunov's direct method with applications by Joseph L Salle and Solomon Lefschetz, Elsevier, 2012.
[29] H. I. Freedman, S. Ruan, M. Tang, Uniform persistence and flows near a closed positively invariant set, Journal of Dynamics and Differential Equations 6 (4) (1994) 583–600.
[30] M. Y. Li, J. R. Graef, L. Wang, J. Karsai, Global dynamics of a seir model with varying total population size, Mathematical biosciences 160 (2) (1999) 191–213.
[31] S. F. Abimbade, S. Olaniyi, O. Ajala, M. Ibrahim, Optimal control analysis of a tuberculosis model with exogenous re-infection and incomplete treatment, Optimal Control Applications and Methods 41 (6) (2020) 2349–2368.
[32] O. S. Akanni, J. O., F. O. Akinpelu, Global asymptotic dynamics of a nonlinear illicit drug use system, J. Appl. Math. Comput. 66 (2021) 39–60.
[33] S. Bowong, J. Tewa, Mathematical analysis of a tuberculosis model with differential infectivity, Communications in Nonlinear Science and Numerical Simulation 14 (11) (2009) 4010–4021.
[34] A. Temgoua, Y. Malong, J. Mbang, S. Bowong, Global properties of a tuberculosis model with lost sight and multi-compartment of latents, Journal of Mathematical Modeling 6 (1) (2020) 47–76.
[35] Worldometer, https://www.worldometers.info/coronavirus/country/ghana/, year = 02-09-2020.
[36] M. Martcheva, Introduction to Mathematical Epidemiology, Vol. 61, Springer, 2015.
[37] W. P., Review total population, https://worldpopulationreview.com/ (2020).
[38] G. H. Service, COVID-19 Updates, Ghana., www.ghanahealthservice.org., [Retrieved 23 July 2020] (2020).
[39] H. H. Publishing., How long can the coronavirus that causes covid19 survive on surfaces, accessed 5th may 2020, https://www.health.harvard.edu/diseases-and-conditions/covid-19-basics, (2020).
[40] J. K. K. Asamoah, F. Nyabadza, Z. Jin, E. Bonyah, M. A. Khan, M. Y. Li, T. Hayat, Backward bifurcation and sensitivity analysis for bacterial meningitis transmission dynamics with a nonlinear recovery rate, Chaos, Solitons & Fractals 140 (2020) 110237.

[41] J. Wu, R. Dhingra, M. Gambhir, J. V. Remais, Sensitivity analysis of infectious disease models: methods, advances and their application, Journal of The Royal Society Interface 10 (86) (2013) 20121018. doi:https://doi.org/10.1098/rsif.2012.1018.